論文 Applicability of One Dimensional Gradient Plasticity in Identifying Fracture Process of Concrete

Khan Mahmud AMANAT [*1] & Tada-aki TANABE [*2]

ABSTRACT: Numerical simulation of concrete fracture process requires a rational formulation of the localized phenomenon keeping the continuity of strain between the localized zone and outside the localized zone. Applicability of gradient plasticity models to capture localization has already been established [1,2]. In this study a one dimensional gradient plasticity model is used to investigate the effect of some parameters on the overall load-deflection response and on localization phenomenon. Also some numerically obtained results are compared with experiments that shows the model's applicability in mode-1 type fracture. It has been shown that one-dimensional formulation is useful to verify test results and to select proper values of model parameters.
KEYWORDS: concrete, fracture, finite element, plasticity, gradient plasticity.

1. INTRODUCTION

Localization of deformation refers to the emergence of narrow regions in a structure where all further deformation tends to concentrate, in spite of the fact that the external actions continue to follow a monotonic loading program. The remaining parts of the structure usually unload and behaves in an almost rigid manner. The phenomenon has a detrimental effect on the integrity of the structure and often acts as a direct precursor to structural failure. It is observed for a wide range of materials, including rocks, concrete, soils, metals, alloys and polymers, although the scale of localization in the various materials may differ by some orders of magnitude. In simulating localized fracture process of concrete classical continuum models are applicable only when the degree of material heterogeneity is small compared to the size of the specimen. In such cases the presence of microcracks and microvoids can be neglected and the stress and strain can be treated as averaged values. But when the scale of material heterogeneity becomes comparable with the size of the specimen, like when macro-cracks develops, classical continuum models reach the limit of their applicability. To solve this problem one can resort to damage evolution in a discontinuous manner like incorporating discrete cracks provided one knows the development of crack patterns beforehand and such formulations are difficult to generalize.

De Borst et al [1] developed an enhanced continuum model in which the failure function is made to depend on the second-order spatial gradient of a fracture strain measure. The theory preserves well-posedness of the governing equations during strain localization and therefore the fracture strain fields remain continuous. The theory includes an additional parameter called internal length scale related to the width of the fracture band. Such gradient-dependent formulation of the concrete material permits localization of deformation without the loss of ellipticity of the governing differential equations. As a direct consequence, in computational

*1 Graduate Student, Department of Civil Engineering, Nagoya University, Member of JCI.
*2 Department of Civil Engineering, Nagoya University, DR, Member of JCI.

analyses a description of the finitely sized fracture process zone is no longer determined by the finite element mesh, i.e. no influence by element size or element orientation can be noticed. Before we apply such a model on a real structure, it is necessary to understand the behavior of different model parameters on concrete fracture process. Structural concrete exhibits non-linear strain softening due to non-homogeneous deformations resulting from macroscopic cracking [6]. It shows some ductility, because the faces of cracks are connected by grain bridges, which delay crack propagation and opening. With the use of a nonlinear description of concrete strength degradation the influence of various model parameters are studied in this paper. Afterwards the applicability of the model is investigated by comparing numerically obtained results with those of experiments found in literature[4, 5].

2. FIELD EQUATIONS AND FINITE ELEMENT APPROACH

Here a brief description of the field equations of gradient plasticity [1] is presented. First we consider the following set of field equations:

$$\mathbf{L}^{\mathrm{T}}\dot{\sigma} = 0, \tag{1}$$

$$\dot{\varepsilon} = \mathbf{L}\dot{\mathbf{u}}, \tag{2}$$

$$\dot{\sigma} = \mathbf{D}\left(\dot{\varepsilon} - \dot{\lambda}\frac{\partial f}{\partial \sigma}\right), \qquad \dot{\lambda} \geq 0, \tag{3}$$

$$f\left(\sigma, \kappa, \nabla^2\kappa\right) = 0 \tag{4}$$

In the above equations $\mathbf{L}$ is a differential operator matrix, $\dot{\sigma}$ and $\dot{\varepsilon}$ are the stress and strain rate tensors respectively, $\dot{\mathbf{u}}$ is a displacement rate vector, $\mathbf{D}$ is the elastic stiffness matrix, $\dot{\lambda}$ is a multiplier being a measure of inelastic flow intensity, f is the gradient dependent failure surface and κ is an invariant measure of fracture strain or damage. In the gradient plasticity formulation it is assumed that $\dot{\kappa} = \eta\dot{\lambda}$ where η is a positive constant. In the following derivation η is assumed to be 1.0 for simplicity although later different values of η were used with necessary changes in the formulation.

The gradient dependence of the failure function makes the fracture flow consistency condition $\dot{f} = 0$ to become a differential equation with second order terms,

$$\mathbf{n}^{\mathrm{T}}\dot{\sigma} - h\dot{\kappa} + g\nabla^2\dot{\kappa} = 0 \tag{5}$$

with the notations,

$$\mathbf{n} = \frac{\partial f}{\partial \sigma} \quad , \quad h = \frac{\partial f}{\partial \kappa} \quad , \quad g = \frac{\partial f}{\partial \nabla^2 \kappa} \tag{6}$$

Therefore, the inelastic strains are discretized using the same mesh of the finite elements as used for the discretization of displacements. For finite element formulation an incremental-iterative algorithm is presented by de Borst et. al. [1] , which requires a weak satisfaction of the equilibrium condition (eq.1) and the failure condition (eq.4) at the end of iteration j+1 of the current loading step, which results in the following two variational equations:

$$\int_V \delta\boldsymbol{\varepsilon}^{\mathrm{T}}\mathbf{D}(\mathrm{d}\boldsymbol{\varepsilon} - \mathrm{d}\lambda\mathbf{n})\,\mathrm{d}V = \int_S \delta\mathbf{u}^{\mathrm{T}}\mathbf{t}_{j+1}\,\mathrm{d}V - \int_V \delta\boldsymbol{\varepsilon}^{\mathrm{T}}\sigma_j\,\mathrm{d}V \tag{7}$$

and,

$$\int_V \delta\lambda\left[\mathbf{n}^{\mathrm{T}}\mathbf{D}\,\mathrm{d}\boldsymbol{\varepsilon} - \left(h + \mathbf{n}^{\mathrm{T}}\mathbf{D}\mathbf{n}\right)\mathrm{d}\lambda + g\nabla^2(\mathrm{d}\lambda)\right]\mathrm{d}V = -\int_V \delta\lambda\, f\left(\sigma_j, \kappa_j, \nabla^2\kappa_j\right)\mathrm{d}V \tag{8}$$

In the above equations d indicates an increment. In equations (7) and (8) only first derivatives of $\mathbf{u}$ appears whereas for λ second derivatives appear. Therefore $\mathbf{u}$ is discretized using linear C^0 shape functions $\mathbf{N}$ and λ is discretized using Hermitian C^1 shape functions $\mathbf{h}$.

$$\mathbf{u} = \mathbf{N}\mathbf{a}, \qquad \lambda = \mathbf{h}^{\mathrm{T}}\Lambda \tag{9}$$

where **a** is nodal displacement vector and Λ is a vector of nodal degrees of freedom for λ. Using a strain nodal displacement matrix **B** = **LN** and a vector **p** containing Laplacians of the shape functions **h** we obtain,

$$\varepsilon = \mathbf{Ba}, \qquad \nabla^2\lambda = \mathbf{p}^T\Lambda \tag{10}$$

Substituting identities (9) and (10) in equations (7) and (8) and requiring that these equations hold true for any admissible value of $\delta\mathbf{a}$ and $\delta\Lambda$, we obtain the following set of matrix equation,

$$\begin{bmatrix} \mathbf{K}_{aa} & \mathbf{K}_{\lambda a}^T \\ \mathbf{K}_{\lambda a} & \mathbf{K}_{\lambda\lambda} \end{bmatrix} \begin{bmatrix} d\mathbf{a} \\ d\Lambda \end{bmatrix} = \begin{bmatrix} \mathbf{f}_e + \mathbf{f}_a \\ \mathbf{f}_\lambda \end{bmatrix} \tag{11}$$

where $\mathbf{K}_{aa}$ is the elastic stiffness matrix, $\mathbf{f}_e$ is the external force vector and $\mathbf{f}_a$ is the nodal forces equivalent to internal stresses defined conventionally. The off-diagonal matrix $\mathbf{K}_{\lambda a}$ and the gradient dependent matrix $\mathbf{K}_{\lambda\lambda}$ are defined as,

$$\mathbf{K}_{\lambda a} = -\int_V \mathbf{h}\mathbf{n}^T\mathbf{D}\mathbf{B}\,dV, \qquad \mathbf{K}_{\lambda\lambda} = \int_V \left[\left(h + \mathbf{n}^T\mathbf{D}\mathbf{n}\right)\mathbf{h}\mathbf{h}^T - g\,\mathbf{h}\mathbf{p}^T\right]dV \tag{12}$$

and the vector of residual forces $\mathbf{f}_\lambda$ due to inexact fulfillment of the fracture condition reads,

$$\mathbf{f}_\lambda = \int_V f\left(\sigma_j, \kappa_j, \nabla^2\kappa_j\right)\mathbf{h}\,dV \tag{13}$$

3. MATERIAL MODEL

In this paper we are dealing with one-dimensional mode-1 fracture problem. So the simple Rankine failure surface is adopted. The failure surface is of the form,

$$f\left(\sigma, \kappa, \nabla^2\kappa\right) = \sigma - \bar{\sigma}_g\left(\kappa, \nabla^2\kappa\right) \tag{14}$$

where σ is the axial stress and $\bar{\sigma}_g$ is the yield strength which depends on both κ and $\nabla^2\kappa$. Since κ is a measure of the degree of fracture process, it is assumed that $d\kappa = d\varepsilon^p$ where $d\varepsilon^p$ is the fracture strain defined as,

$$d\varepsilon^p = \frac{df}{d\sigma} \tag{15}$$

The form of $\bar{\sigma}_g$ adopted in this paper is,

$$\bar{\sigma}_g = \bar{\sigma}_t(\kappa) - g(\kappa)\nabla^2(\kappa) \tag{16}$$

where $\bar{\sigma}_t(\kappa)$ is a given standard softening rule and $g(\kappa)$ is a given gradient influence function. Experimental evidence shows a nonlinear softening behavior of concrete in tension [5]. When concrete fails in tension it typically leads to a sudden discontinuity at peak strength with a very brittle appearance of the load-deformation response. For this reason an exponentially decreasing non-linear softening rule similar to that shown in Fig.1 is adopted where,

$$\bar{\sigma}_t = \bar{\sigma}_t\left(\kappa, f_t, \kappa_u\right) \tag{17}$$

in which f_t and κ_u are uniaxial tensile strength and ultimate value of equivalent fracture strain respectively. The hardening modulus h is then obtained as,

$$h = \frac{\partial f}{\partial \kappa} = \frac{\partial \bar{\sigma}_g}{\partial \kappa} = \bar{\sigma}_t'(\kappa) - g'(\kappa)\nabla^2(\kappa) \tag{18}$$

where the Laplacian is treated as an independent variable during differentiation and third order terms are neglected. Using the analytical solution obtained by Borst et. al. [1] we can relate h with $g(\kappa)$ via internal length scale l as

$$g(\kappa) = -l^2 \bar{\sigma}_t'(\kappa) \qquad (18)$$

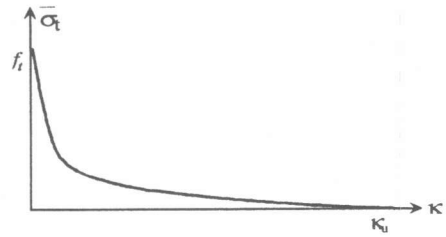

Fig. 1. Standard tensile softening rule

4. NUMERICAL STUDY

As stated before, in order to get an insight into the behavior of the gradient-dependent plasticity model a rigorous numerical study was made with different values of model parameters. For the purpose of study a bar under uniaxial tension is considered. The length of the bar is L = 100 mm with a unit cross sectional area. The initial values of other parameters are, modulus of elasticity E = 20000 N/mm^2 , tensile strength f_t = 3 N/mm^2, internal length scale l = 5 mm, ultimate value of equivalent fracture strain κ_u= 0.01 and η = 1.0. Later different values of κ_u and η are taken to see their effect. The solid lines of Fig.2a and Fig.2b show the load-deformation diagram and distribution of total strain along the length of the bar respectively for the initial values of the parameters. The results correspond to mesh size of 40 elements with a relatively denser mesh at central region. To trigger localization at the center of the bar only four elements at the center of the bar (covering approximately 4 mm length at center) were made weak by reducing tensile strength by 10%. However, as the amount of plastic strain increased during loading process more and more adjacent elements entered into localization process due to gradient effect until a steady state condition was reached finally. Fig.2a also shows the effect of different values of κ_u on the overall load-deformation process and Fig.2b shows the same on strain distribution. From Fig.2a it is clear that smaller values of κ_u make the load-deformation behavior more brittle in addition to lowering the load at ultimate end displacement. This is because lower value of κ_u implies smaller value of fracture energy for same value of strength as it can be seen from the softening diagram. But its effect on growth of localization is not much significant as observed from Fig.2b. Smaller values of κ_u only make a slight decrease on the growth of plasticity. Similar results are obtained for the variation of η and the results are shown in Fig.3a and Fig.3b. No appreciable effect of η is noticed on the localized strain distribution as revealed from Fig.3b. But

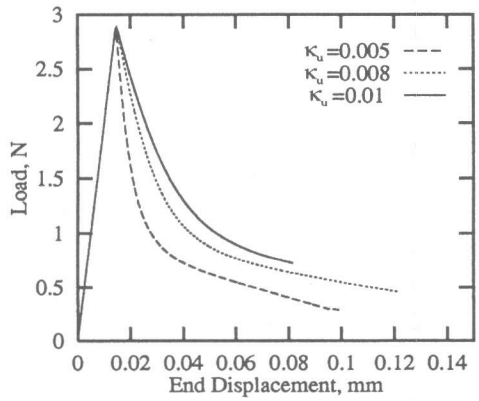

Fig.2a Effect of κ_u on load-displacement

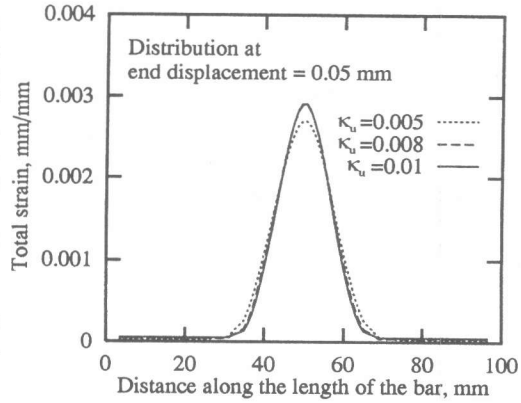

Fig.2b Effect of κ_u on distribution of total strain

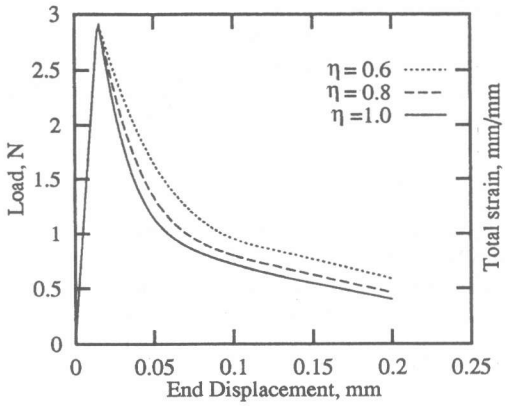

Fig.3a. Effect of η on load-displacement

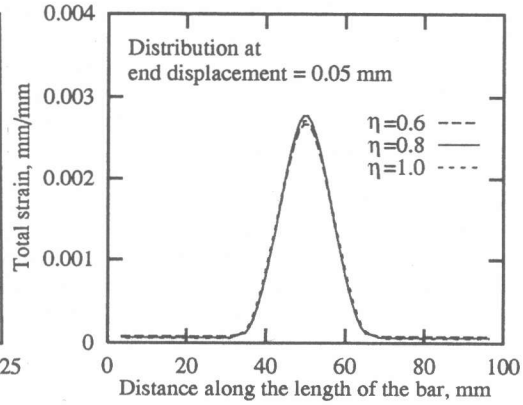

Fig.3b Effect of η on distribution of total strain

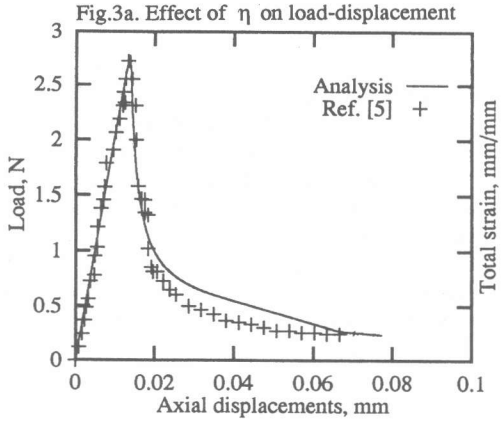

Fig.4a Comparison of load-displacement response between analysis and test data of ref. [5]

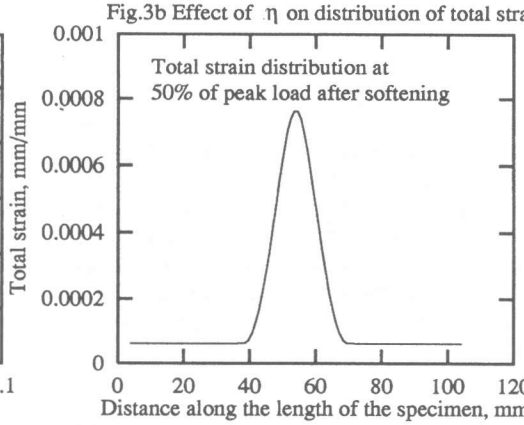

Fig.4b Strain distrbution obtained for test sample of ref.[5]

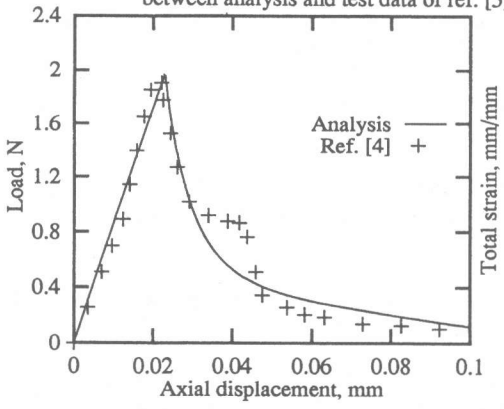

Fig.5a Comparison of load-displacement response between analysis and test data of ref. [4]

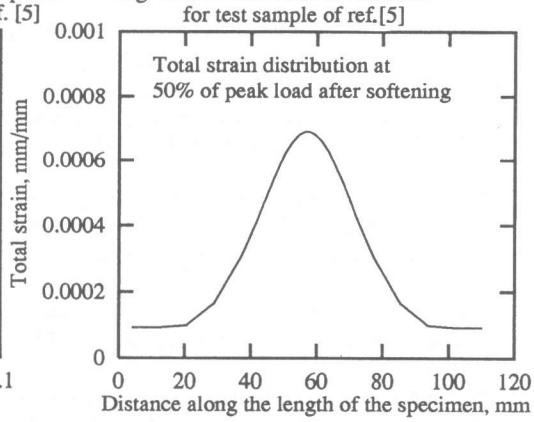

Fig.5b Strain distrbution obtained for test sample of ref. [4]

unlike κ_u, smaller values of η has the effect of flattening the load-displacement response (Fig.3a). The accumulation of κ depends on the growth of λ and these two quantities are related via η. Smaller values of η slows down the accumulation of κ and hence it decreases the strength degradation rate thereby making the post-peak response more ductile. No appreciable effect of η is noticed on the localized strain distribution as revealed from Fig.3b. Thus it can be inferred that smaller values of η or higher values of κ_u will result in higher values of fracture energy.

To assess the effectiveness of current formulation, it was tried to reproduce test results numerically for the one-dimensional case. Fig.4a compares the numerically obtained load-deformation diagram with that obtained by experiment by William et. al. [5]. Due to the lack of sufficient data the value of initial Young's modulus was determined from the experimentally obtained load-displacement diagram. The values of different parameters used are , length of the bar L = 107 mm, Young's modulus E = 22100 N/mm^2 , ultimate value of equivalent fracture strain κ_u = 0.0035, η = 1.0 and internal length l= 5 mm. Fig.5a shows similar comparison for a test on mortar specimen reported by Chen [4]. For this simulation L = 114.3 mm, E = 9850 N/mm^2, κ_u = 0.0035, η = 1.2 and l = 12 mm. Fig.4b and Fig.5b shows corresponding strain distribution along the length of the bar which are obtained numerically. Both from Fig.4a and Fig.5a a fairly good agreement between experiment and numerical analysis is found though at later stage of loading process a little overestimation of strength by numerical analysis is observed. Fig.5b shows a wider localization band than that of Fig.5a. This is due to taking of a larger value of l (12mm) for the later case.

5. CONCLUSION

The applicability of one dimensional gradient plasticity formulation for non-linear softening behavior of concrete in tension is demonstrated. Although one dimensional formulation has limited application, comparison with test results indicates the potential of gradient dependent formulation in capturing localization with strain continuity and shows its usefulness in verifying experimental results. The examples show that with a careful selection of parameters, the model can be successfully applied to simulate fracture process of concrete. It was observed that post peak response is independent of the formation of localization band. However it is obvious that the choice of a particular softening diagram governs the shape of non-linear post peak response. Hence a careful choice of softening diagram is necessary to successfully trace the experimental results.

REFERENCES

1. De Borst R. and Mühlhaus H. B., "Gradient-Dependent Plasticity: Formulation and Algorithmic Aspects", Int. J. Num. Meth. Eng., 35, 1992, pp. 521-639.

2. Mühlhaus H. B. and Aifantis E.C., "A Variational Principle for Gradient Plasticity", Int. J. Solids Structures, 28, 1991, pp. 845-857.

3. De Borst R., Mühlhaus H. B. and Pamin J, "A Gradient Continuum Model for Mode-I Fracture in Concrete and Rock", Fracture Mechanics of Concrete Structures, Ed Z.P. Bazant, Elsevier, London & New York, 1992, pp. 252-259.

4. Chen W. F. and Yamaguchi E., "On Constitutive Modelling of Concrete Materials", Seminar On F.E.M. Analysis Of Concrete Structures", JCI, Tokyo, May 1985

5. William K., Hurlbut B. and Sture S., "Experimental, Constitutive and Computational Aspects of Concrete Failure", Seminar on F.E.M. Analysis of Concrete Structures, JCI, Tokyo, May 1985

6. Lokuliyana D.R. and Tanabe T., "Fracture Mechanics Based Analysis of Thermal Crack Propagation of Massive Concrete", NUCE Research Report No. 9202, Dept. of Civil Engg., Nagoya University, Japan, July 1992.